Electrophysiological Model of Intact and Processed Plant Tissues: Cell Disintegration Criteria

ARTICLE *in* BIOTECHNOLOGY PROGRESS · DECEMBER 1998

Impact Factor: 2.15 · DOI: 10.1021/bp990079f · Source: PubMed

Electrophysiological Model of Intact and Processed Plant Tissues: Cell Disintegration Criteria

Alexander Angersbach, Volker Heinz, and Dietrich Knorr*

Department of Food Biotechnology and Food Process Engineering, Berlin University of Technology, Königin-Luise-Strasse 22, D-14195 Berlin, Germany

Frequency versus conductivity relationships of food cell system, based on impedance measurements as characterized by polarization effects of the Maxwell−Wagner type at intact membrane interfaces, are presented. The electrical properties of a biological membrane (represented as a resistor and capacitor) are responsible for the dependence of the total conductivity of the cell system on the alternating current frequency. Based on an equivalent circuit model of a single plant cell, the electrical conductivity spectrum of the cell system in intact plant tissue (potato, carrot, banana, and apple) was determined in a frequency range between 3 kHz and 50 MHz. The electrical properties of a cell system with different ratios of intact/ruptured cells could also be predicted on the basis of a description of a cell system consisting of elementary layers with regularly distributed intact and ruptured cells as well as of extracellular compartments. This simple determination of the degree of cell permeabilization (cell disintegration index, p_o) is based upon electric conductivity changes in the cell sample. For accurate calculations of p_o, the sample conductivities before and after treatment, obtained at low- (f_l) and high-frequency (f_h) ranges of the so-called β-dispersion, were used. In this study with plant cell systems, characteristic conductivities used were measured at frequencies $f_l = 3$ kHz and $f_h = 12.5$ MHz. The disintegration index was used to analyze the degree of cell disruption after different treatments (such as mechanical disruption, heating, freeze−thaw cycles, application of electric field pulses, and enzymatic treatment) of the plant tissues.

Introduction

During processing or storage of cellular foodstuffs, attention needs to be given to the degree of disintegration of the initial tissue structure because of its impact on food quality, functionality, deterioration, and safety.

Due to the inhomogeneous structure of biological cells and tissues, the analysis of electrophysical properties of intact or processed tissues represents a detailed view of the cellular nature of the sample under consideration. In addition, the evaluation of cell cultures proved to be a valuable tool to examine and monitor processing effects on plant systems (*1*). Generally, the compartments of a cell are separated from the surrounding medium by a cell membrane, which consists mainly of highly structured, electrically insulating phospholipids. As long as the media on both sides of the cell membrane are electrically conductive, the macroscopic tissue system will show complex conductivity, which is dependent on the frequency of the current applied.

The behavior of biological tissue or suspended cells exposed to an alternating electrical field can be described using Maxwell's (*2*) and Wagner's (*3*) theory of heterogeneous dielectrics. Modifications of this basic concept were applied to biological, biochemical, or biomedical problems (*4*−*10*). In the field of plant physiology, electrical impedance analysis was used to detect freezing injury (*11*, *12*), cold adaptation (*13*, *14*), or infection by viruses (*15*).

A few methods were also described to estimate the quality and freshness of fish and animal tissue using empirical relationships between the electrical properties and the sample condition in the small-frequency region. The indexes derived were fitted quite closely to other commonly used analyses of the quality parameters (*16*−*19*).

This paper summarizes some of our activities on an impedance approach for detecting cell disintegration with high accuracy and for being able to process biological cells/tissues to prespecified degrees of permeabilization.

Theoretical Considerations

The presence of intact membranes with very low electrical conductance in a cellular sample (with conductive inner and outer phases) produce alternating current (AC)-frequency-dependent changes of the macroscopically detectable electrical conductivity. According to Schwan (*20*), the so-called β-dispersion is the result of the repeated charging process of the membranes in the altering electrical field. For biological systems, it is more pronounced in a frequency range between 1 kHz and 100 MHz (*10*, *20*, *21*). The β-dispersion may be regarded as a special case of the Maxwell−Wagner polarization effect, which generally explains the frequency behavior of the impedance due to the presence of nonconductive interfaces separating two conductive aqueous phases, such as a dielectric in a parallel plate capacitor (*6*, *22*). Therefore, in an equivalent circuit, the electrical behavior of the cell membrane can be assumed as a capacitor connected with

* Corresponding author. Tel.: +49 30 314 71250. Fax: +49 30 832 7663. E-mail: foodtech@mailszrz.zrz.tu-berlin.de.

10.1021/bp990079f CCC: $18.00
Published on Web 07/13/1999

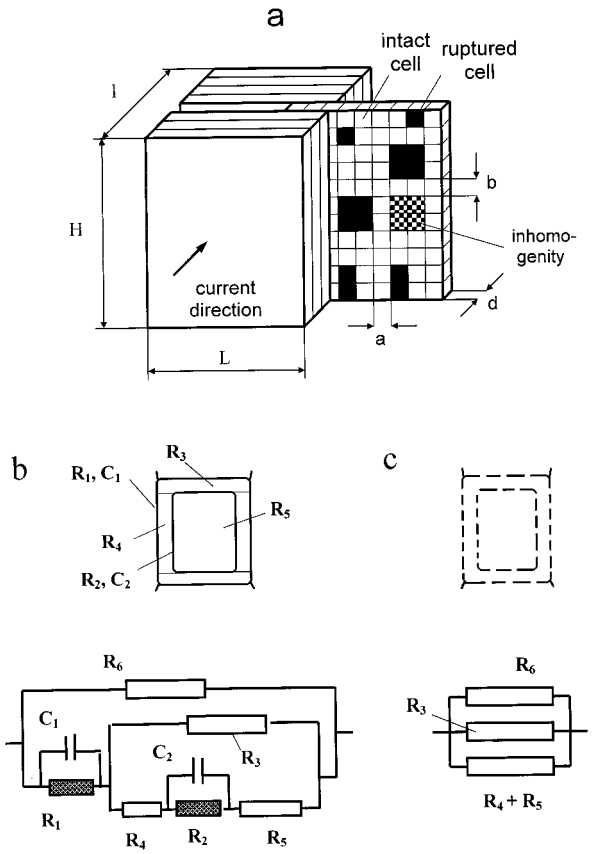

Figure 1. Schematic diagram of elementary layers in cell tissue systems (a); equivalent circuit model of the intact (b) and ruptured (c) plant cells. R_1, R_2, plasma and vacuole membrane (tonoplast) resistance; C_1, C_2, plasma and vacuole membrane (tonoplast) capacitance; R_3, cytoplasmic resistance surrounding the vacuole in the direction of current; R_4, cytoplasmic resistance in vacuole direction; R_5, resistance of the vacuole interior; R_6, resistance of the extracellular compartment.

one resistor in parallel. The liquid phases on both sides of a membrane can be introduced to this circuit as two additional series resistors. Within the frequency band relevant for β-dispersion, the dielectric current is small compared to the resistive current determined by the electrical conductivities. At higher frequencies (greater than approximately 0.1−0.2 GHz), dipole rotation of molecules in biological solution will further influence the complex conductivity (*10, 23*). An approximation of an elementary cell within a tissue consisting of extracellular compartments, cytoplasma membrane, cytoplasma, tonoplast, and vacuole yields a more complex equivalent electrical circuit (Figure 1b). Similar circuits were frequently used in plant physiology for the purpose of impedance analysis (*11*−*14, 24, 25*).

The complete rupture of the cytoplasma membrane and the tonoplast of plant cells reduces the equivalent electrical circuit to a parallel connection of three ohmic resistors, formed by the electrolytes of the cytoplasma, the vacuole, and the extracellular compartments, respectively (Figure 1c). The tissue inhomogeneities (such as gas vacuoles or oil droplets in raw or processed material) are to be added to the equivalent circuit as ohmic resistors (as far as charge polarization can be excluded).

The frequency-dependent electrical conductivity of a tissue system may be defined as

$$\sigma(\omega)^{s} = \frac{1}{A|Z(j\omega)^{s}|} \tag{1}$$

where l is the length of the sample, A is the area perpendicular to the electrical field, and $Z(j\omega)^{s}$ is the system impedance, where $\omega = 2\pi f$ is the angular frequency. While taking into account the equivalent circuit of one elementary cell (Figure 1b), the tissue sample can be regarded as multiple connections in series and in parallel of numerous basic units. The schematic view in Figure 1a presents the sample of length l composed of n layers (in series) of thickness d. Each layer consists of m individual cells (in parallel), with average area $A_C = ba$, which are in the total exposed area ($A = HL$) perpendicular to the electric field. The model considered here is valid if the intact and ruptured cells as well as inhomogeneities in initial intact and processed cell systems are regularly distributed.

Using this approximation, the impedance of a tissue sample containing different portions of intact and ruptured cells as well as noncellular compartments can be represented by eq 2,

$$Z(j\omega)^{s} = \frac{n}{m}\left[\frac{i}{Z(j\omega)^{s}} + \frac{p}{Z^{p}} + \frac{g}{Z^{g}}\right]^{-1} \tag{2}$$

where i and p are the ratios of intact and ruptured cells to the total number of cells in an elementary layer, g is the ratio of the inhomogenity inclusion unit to the total number of cells in an elementary layer, $i + p + g = 1$, Z^{g} is the resistance of additional intracellular volume elements, and Z^{p} is the resistance of the elementary unit with ruptured membranes and can be expressed as eq 3,

$$Z^{p} = \frac{(R_4 + R_5)R_3R_6}{(R_4 + R_5)(R_3 + R_6) + R_3R_6} \tag{3}$$

where R_3 represents the cytoplasmic resistance surrounding the vacuole in the direction of the electrical field, R_4 represents the cytoplasmic resistance covering vacuole in direction of the electrical field, R_5 is the resistance of the vacuole interior, and R_6 is the resistance of the extracellular compartment.

$Z(j\omega)^{i}$ is the complex impedance of one elementary unit with intact membranes and can be represented as eq 4,

$$Z(j\omega)^{i} = \frac{R_6[Z(j\omega)_1 + Z(j\omega)_{c+v}]}{R_6 + Z(j\omega)_1 + Z(j\omega)_{c+v}} \tag{4}$$

where $Z(j\omega)_1$ is the complex impedance of cytoplasma membrane, which can be expressed as eq 5,

$$Z(j\omega)_1 = \frac{R_1[-jX_1(j\omega)]}{R_1 - jX_1(j\omega)} \tag{5}$$

where $X_1(j\omega)$ is equal to $(2\pi fC_1)^{-1}$, R_1 and C_1 are the resistance and capacitance of cytoplasma membrane, f is the measurement frequency, j is equal to $(-1)^{1/2}$, and $Z(j\omega)_{c+v}$ is the complex impedance of cytoplasma, including vacuole and tonoplast, and can be expressed as eq 6,

$$Z(j\omega)_{c+v} = \frac{R_3[R_4 + R_5 + Z(j\omega)_2]}{R_3 + R_4 + R_5 + Z(j\omega)_2} \tag{6}$$

$Z(j\omega)_2$ is the complex impedance of tonoplast:

$$Z(j\omega)_2 = \frac{R_2[-jX_2(j\omega)]}{R_2 - jX_2(j\omega)} \tag{7}$$

where $X_2(j\omega)$ is equal to $(2\pi fC_2)^{-1}$, and R_2, and C_2 are the resistance and capacitance of tonoplast.

For homogeneous samples consisting of intact cells only ($i = 1$; $p = 0$; $g = 0$), eq 2 can be simplified to

$$Z(j\omega)^{s} = \frac{nZ(j\omega)^{i}}{m} \tag{8}$$

The rearrangement of eq 8 using $m = A/A_c$ and $n = l/d$ yields

$$Z(j\omega)^{s} = \frac{A_c}{A}\frac{l}{d}Z(j\omega)^{i} \tag{9}$$

This implies that the impedance of the intact tissue is a linear function of the impedance of one elementary unit. The slope of this function comprises the geometrical aspects of the sample under consideration. Due to this fact, the specific conductivity of tissue sample containing intact cells, $\sigma(\omega)^{s}$, and the specific conductivity of the elementary unit with intact membranes, $\sigma(\omega)^{i}$, are equal.

The results of numerous experiments indicate that the conductivity−frequency spectra of intact and processed plant tissue in a range between 1 kHz and 50 MHz can typically be divided into characteristic zones (*26*). An evaluation of the conductivity spectra of processed samples also has a typical character. The increase in conductivity of processed samples in low-frequency ranges is the result of cell membrane rupture, which has a very high resistance and reactance in this frequency range. In the high-frequency range, the conductivities of intact cells and of cells with ruptured membranes are practically not different. This can be explained by the fact that, within this frequency range, the intact cell membrane has a negligible impedance (membrane reactance $X_1(j\omega)$; $X_2(j\omega) \rightarrow 0$). A decrease in the difference of conductivity in high- and low-frequency ranges in β-dispersion is the result of cell rupture.

The curves a and b in Figure 2 are examples for the conductivity response in the specific β-dispersion frequency band of materials which contain biological membranes surrounded by conductive fluids (*8, 10, 22, 27, 28*). The impedance behavior of cell systems at extremely low (f_l) or high (f_h) frequencies can be approximated by

$$\frac{dZ(j\omega)^{s}}{df} = 0 \qquad \text{and} \qquad \frac{dZ(j\omega)^{i}}{df} = 0 \tag{10}$$

Hence, the impedance of a single intact cell, $Z(j\omega)^{i}$, is equal to the product of the ohmic resistances of the basic circuit, if the specific conductivity of the membrane is much lower than the conductivities of the neighboring fluids. The imaginary component of the plant cells' impedance equals zero within the range of β-dispersion at frequencies $f_l < 5$ kHz and $f_h > 5$ MHz. In the case of extremely low and extremely high frequencies, the calculation of the impedance of the equivalent circuit of the basic cell unit can be approximated as follows:

at f_l ($f \rightarrow 0$ and $X_1(j\omega)$; $X_2(j\omega) \rightarrow \infty$; $R_3 \ll R_1$):

$$Z_l^{i} = \frac{R_1R_6}{R_1 + R_6} \tag{11}$$

at f_h ($f \rightarrow \infty$ and $X_1(j\omega)$; $X_2(j\omega) \rightarrow 0$):

$$Z_h^{i} = \frac{(R_4 + R_5)R_3R_6}{(R_4 + R_5)(R_3 + R_6) + R_3R_6} \tag{12}$$

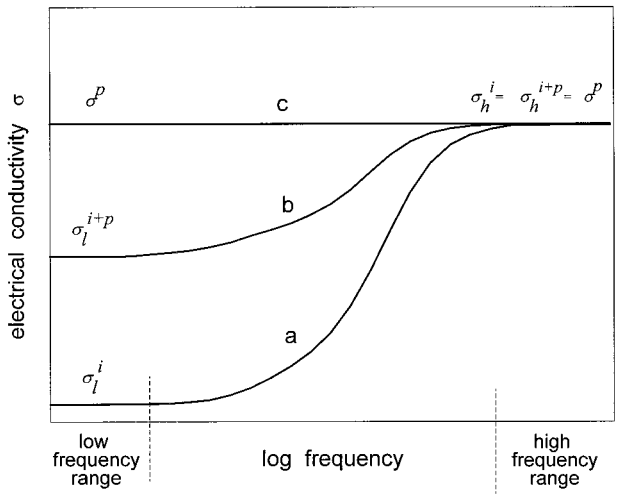

Figure 2. Typical conductivity spectra in frequency range from single kilohertz to tens of megahertz of biological tissue with intact cells (a), intact + ruptured cells (b), and total ruptured cells (c).

As discussed earlier, the impedance of an elementary tissue unit with ruptured membranes (Z^p) and of extracellular compartments (Z^g) does not show any frequency dependence. Hence, at low frequencies, the calculation of the specific conductivities of intact and ruptured cells and inhomogeneous units can be given as

$$\sigma_l^{i} = \frac{d}{A_cZ_l^{i}} \tag{13}$$

$$\sigma^{p} = \frac{d}{A_cZ^{p}} \tag{14}$$

$$\sigma^{g} = \frac{d}{A_cZ^{g}} \tag{15}$$

For a tissue sample that consists of certain portions of intact and ruptured cells together with intercellular inhomogeneities, eqs 13−15 can be combined for lower frequency range as given below:

$$\sigma_l^{s} = i\sigma_l^{i} + p\sigma^{p} + g\sigma^{g} \tag{16}$$

Elimination of factor i as a measure of the portion of intact cells and rearrangement of eq 16 yields the ratio of ruptured cells, p, as a function of conductivity:

$$p = \frac{\sigma_l^{s} + g(\sigma_l^{i} - \sigma^{g}) - \sigma_l^{i}}{\sigma^{p} - \sigma_l^{i}} \tag{17}$$

For the purpose of process evaluation, it is important to know the magnitude of cells in a tissue sample affected by the treatment. Hence, an index of disintegration, p_o, can be introduced, which comprises of the number of ruptured cells relative to the initially intact cells and independent of the portion g of tissue inhomogeneity due to extracellular compartments. The index of disintegration can be presented as

$$p_o = \frac{p}{(1 - g)} \tag{18}$$

In cases where the resistance of the extracellular compartments is infinitely high (e.g., gas bubbles produced during mashing of vegetable tissue), $\sigma^{g} = 0$. Substituting

the value of p_o from eq 17 into eq 18 gives

$$p_o = \frac{\sigma_l^t - (1-g)\sigma_l^i}{(1-g)(\sigma^p - \sigma_l^i)} \quad (19)$$

The disintegration index of tissue without extracellular compartments ($g = 0$ and $p_o = p$) can be obtained by eq 20:

$$p_o = \frac{\sigma_l^t - \sigma_l^i}{\sigma^p - \sigma_l^i} \quad (20)$$

The direct measurement of specific conductivity, σ^p, of ruptured cells in a tissue sample (which is necessary for the calculation of p_o) is not possible with conventional measurement techniques. However, comparison of eqs 3 and 12 yields σ^p, which is replaced (eq 20) by the complex conductivity of intact cells at high frequency (σ_h^i) measured within the high-frequency range:

$$\sigma^p = \sigma_h^i = \sigma_h^s \quad (21)$$

Due to possible processing effects which coincide with cell rupture, such as changes in temperature, tissue porosity, and electrolyte concentration, the estimation of p_o with eq 20 using the approximation of eq 21 might not be accurate. A vivid example of the change in conductivity due to a sample temperature increase is presented by the conductivity spectra measured immediately after application of one high electric field pulse (see Figure 7a). Hence, a factor k was introduced, which offers a suitable correction as a function of the above-mentioned effecting variables and is constant for low- and high-frequency ranges:

$$\sigma_{h\,real}^s = k\sigma_h^s = k\sigma_h^i \text{ and } \sigma_{l\,real}^s = k\sigma_l^s \quad (22)$$

Subsequently, the correction has to be considered for the calculation of the cell disintegration index (p_o):

$$p_o = \frac{(\sigma_h^i/\sigma_{h\,real}^s)\sigma_{l\,real}^s - \sigma_l^i}{\sigma_h^i - \sigma_l^i} \quad (23)$$

The parameter p_o ranges from 0 (intact tissue) to 1 (complete membrane rupture). Determination of p_o in a processed sample is carried out by measuring the conductivity of initial intact (σ_l^i and σ_h^i) and treated (σ_{lreal}^s and σ_{hreal}^s) sample at low and high frequencies within the band of β-dispersion.

Materials and Methods

Potatoes (Adritta), carrots, bananas (Columbia), and apples (Jonagold) were purchased from a local market.

High-Pressure Treatment. Apple samples (cylinder: 20 mm diameter, 30 mm long) were treated in a high-pressure vessel (EPSInt, St-Niklaas B) at 50 MPa and 20 °C for 10 min.

Treatment with High-Intensity Electric Field Pulses (HELP). Carrot samples (cylinder: 10 mm diameter, 20 mm long) were treated with a HELP prototype, designed and constructed in our department, with peak field strength $E = 3.2$ kV/cm (exponential voltage decay), pulse duration 1.5 ms, and specific energy input $Q = 10.8$ kJ/kg. The temperatures before and after pulse application were 20 and 23 °C, respectively.

For heat treatment, the potato samples (cylinder: 10 mm diameter, 20 mm long) were heated from 20 to 90 °C in a water bath, and then they were rapidly cooled to room temperature for p_o determination.

For freezing−thawing treatments, the samples were frozen in compartments at different temperatures (0 to −10 °C) for 4 h. The cooling rate was about 5 °C/h. The samples were thawed at room temperature, and then the cell disintegration index p_o was determined.

Mechanical Disruption of the Potato Tissue. The coarsely ground samples (with 42/58% of solid/liquid phases) were prepared by grating the potato into strips with cross-section area of 2.5 mm × 0.6 mm. Fine-grained samples (with particle size of 0.3−0.7 mm) were produced at a ratio of 32/68% of solid/liquid phases.

Enzymatic Treatment. *Pectinex Ultra SP-L* enzyme (Novo Nordisk Ferment Ltd., Switzerland) was added to the apple mash (apple tissue after coarse mechanical crushing, particle size of 3−5 mm) at concentrations of 0.1−20 g/kg. The examined samples were incubated at 20 °C for 5.5 h without stirring.

Impedance Measurement. The electrical conductivity $\sigma(\omega)^s$ for intact and processed samples was obtained from measured impedance according to eq 1. The impedance spectra were determined with impedance measurement equipment (Electronic Manufacture Co., Mahlsdorf, Germany). The phase voltages (square wave geometry) were each of equal amplitude (typically between 1 and 5 V peak to peak), and the frequency was in the range from 3 kHz to 50 MHz.

For potato, carrot, and banana samples (longitudinal, cross section), impedance was measured in a piece of sample with parallel plate disk electrodes (9.7 mm diameter, the distance between the electrodes was 20 mm; the capacitance of the measuring cell was ∼2.0 pF). For apple mash, impedance was measured in a piece of mash with a steel needle electrode (2 mm diameter, 10 mm long, the distance between two needle electrodes was 20 mm; the capacitance of the measuring cell was ∼1.1 pF). The correction for the capacitance and inductance (about 1.2 μH) arising from the measuring cell and feed cable was made using Schwan's method (*29*, *30*).

Calculations. In plant tissue with a density-packed cell system, each cell can be treated approximately as a cube. The relative volume of vacuole within a cell (V) and the relative conductivity (S) can be expressed as

$$V = \frac{V_{vacuole}}{V_{cell}} \quad (24)$$

$$S = \frac{\sigma_{plasma}}{\sigma_{vacuole}} \quad (25)$$

where $V_{vacuole}$ and V_{cell} are the vacuole and cell volumes, and σ_{plasma} and $\sigma_{vacuole}$ are the plasma and vacuole specific conductivities, respectively.

In the high-frequency range, the correlation between intact cell impedance (Z_h^i), vacuole (R_5) and plasma (R_3, R_4) resistances can be demonstrated by eqs 26−28:

$$R_3 = \frac{R_6 Z_h^i [S + V^{1/3}(1-V^{2/3})^{-1} + 2(1-V^{1/3})]}{(R_6 - Z_h^i)[S + 2(1-V^{1/3})]} \quad (26)$$

$$R_4 = R_3(V^{2/3} - V)(1 - V^{2/3}) \quad (27)$$

$$R_5 = R_3 S(V^{-1/3} - V^{1/3}) \quad (28)$$

Tonoplast resistance (R_2) is calculated from the following correlation between plasma membrane resistance (R_1) and the relative volume of the vacuole in the cell:

$$R_2 = R_1 V^{-2/3} \tag{29}$$

Equations 26−29 are derived from correlation among Z^i_h, R_{1-6}, V, and S under the assumption that the vacuole in cubic form is centrally positioned in a cell (Figure 1b).

R_6 is calculated from eq 11 by impedance from intact cell at low frequencies (Z^i_l) under the condition that the extracellular resistance is very low, as is plasma membrane resistance (as approximation $R_6 < 0.01R_1$). The electrical resistances R_3, R_4, and R_5 are calculated from eq 12 and eqs 26−28 using the impedance of intact cells at high frequencies (Z^i_h) and variation of parameters V and S. The characteristic cell impedances Z^i_l and Z^i_h were calculated according to eq 30 using specific conductivities σ^i_l and σ^i_h determined from tissue in the intact state at 3 kHz and 12.5 MHz, respectively:

$$Z^i_l = \frac{d}{A_c \sigma^i_l}; \quad Z^i_h = \frac{d}{A_c \sigma^i_h} \tag{30}$$

By variation of the relative volume V from 0 to 1, of relative conductivity S from 0.5 to 1.5, and of membrane capacities C_1 and C_2 from 1 to 50 pF, the parameters necessary for best fit for rebuilding a measured conductivity spectrum, $\sigma(\omega)^s$, were determined. The procedure for selecting the most appropriate cell parameters V, S, C_1, and C_2 was based on a complex nonlinear least-squares analysis (*31*), which minimizes the differences of sum of squares between experimental data and corresponds to theoretical predictions according to a model.

The inhomogeneity ratio (g) in the apple sample was (to an approximation) defined as the gas space ratio:

$$g = 1 - \frac{\rho_g}{\rho} \tag{31}$$

where ρ_g and ρ are the specific densities of the cell systems with and without gas space, respectively.

Results and Discussion

Evaluation of Properties of Intact Homogeneous Tissue. Frequency-dependent changes in conductivity of intact membranes of potato, carrot, and banana tissues (neglecting gas space within the tissues and $g = 0$) could be used to prove the theory of the electrophysical model described (see Figure 3).

Experimental data accumulated regarding potato tissues (cell size approximately 100 μm) showed significant changes of the relative volume in the vacuole of cells to $V = 0.7$, as well as in relative conductivity to $S = 0.8$ (eqs 24 and 25). The capacitance of the vacuole membrane can reach $C_1 = 35$ pF and that of the tonoplast $C_2 = 20$ pF (Table 1).

Under simplified conditions ($V - 0$, $R_2 - 0$ and $V - 1$, $R_1 - 0$), the present electrical model of an elementary cell with tonoplast and plasma membranes (so-called double shell model (*25*)) could be transformed into a single-shell model with one outer membrane. This commonly simplified single-shell model of a cell is often used for analyzing the impedance data in plant and animal tissue (*14, 19, 24, 32*) and might be sufficiently significant under extreme β-dispersion conditions (lower $f_l = 1-5$ kHz and higher $f_h = 5-30$ MHz frequency) (Figure 3b). But in the frequency range between f_l and f_h (for potato tissue between about 30 kHz and 3 MHz), the predictions made with the single-shell model are not in agreement with experimental data (Figure 3b, curve 1 and 3); i.e., the presence of a vacuole with tonoplast capacitance C_2 is a very significant component in the discussed model circuit of plant cells. Above all, the single-shell model does not give the possibility to obtain changes in the electrical properties caused by the possible separate disruption of the outer (plasma) or vacuole membrane in plant cells.

During processing of plant tissues, damage could possibly occur within either the plasma membrane or the tonoplast, for example by different cold resistances of the tonoplast and the plasma membrane during nonlethal freezing−thawing treatment or by different pressure resistances of the membranes (*11, 33, 34*). In addition, high-intensity electric field pulse treatment could initiate separate permeabilization of the plasma membrane or the tonoplast (*35*). The electrophysical model allows us to incorporate possible local cell damage into data analysis by calculating R_1, C_1 or R_2, C_2.

Properties of Inhomogeneous Tissues. Apple tissue is a typical example of an inhomogeneous intact tissue and could, consequently, serve as an attractive model for cell structure examination. Nevertheless, experimental data on the impedance analysis of apple tissue in plant physiology are scarce since the models commonly used are not applicable for inhomogeneous tissue.

The inhomogenity of apple tissue can be demonstrated by gas space data, and Figure 4 shows the measured and model-fitted frequency−conductivity curves of intact apple tissue. Experimental data show the specific density of fresh tissue at $\rho_g = 830$ kg/m^3 and the specific density of apple puree without gas space (totally ruptured and evacuated apple tissue) at $\rho = 1052$ kg/m^3. Accordingly, the inhomogenity ratio was at $g = 0.21$ (eq 31). The theoretical conductivity spectrum of the intact tissue (curve b in Figure 4) is based on the proposed model described with $p = 0$, $g = 0.21$ and the resistance of the inhomogenity elements (gas space) $Z_g \rightarrow \infty$ (eq 2).

The theoretical frequency−conductivity behavior for intact apple tissue without gas space (Figure 4, curve d) is based on electrical parameters determined in fresh apple tissue (Table 1) and inhomogenity ratio $g = 0$. Here, the experimental data from compact apple tissue after high hydrostatic pressure treatment can be used as a comparison with the modulated behavior (Figure 4, curve c). During high-pressure treatment at 50 MPa, apple tissue was condensed to a specific density of $\rho = 1010$ kg/m^3. The individual cells do not disrupt under pressures less than 75 MPa. Pressures above 75 MPa cause irreversible cell membrane disruption of apple tissue, and the cell disintegration index p_o increases. Agreement of the predicted curve d and the experimental curve c (Figure 4) is attainable if the capacitances C_1 and C_2 per cell from fresh apple tissue would be increased from values of 18 and 10 pF to 22 and 14 pF, respectively. These results indicate that high-pressure treatment reduces the gas space and compresses the extracellular space. As a result, volume-related biomass concentration increases.

The basic electrical properties of the electrophysical model are shown in Table 1. However, electrical parameters (resistance and capacitance) depend heavily on the origin of the samples (i.e., variety and level of maturity). They are also affected by assumed average cell size. The data used for cell parameters, such as membrane thick-

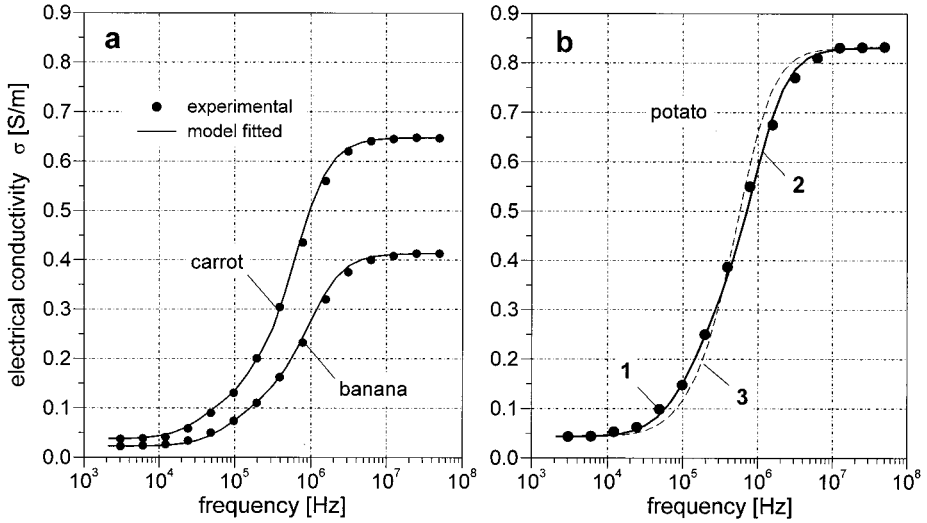

Figure 3. Measured and model-fitted conductivity spectra of intact plant tissue: (a) carrot and banana tissue and (b) potato tissue. The experimental conductivities, σ_l^i and σ_h^i, determined at 3 kHz and 12.5 MHz, respectively, are used for calculation of model-fitted spectra. Potato tissue: Points 1 present the experimental data; curve 2 is calculated with best-fit parameter for double-shell model with vacuole volume ratio $V = 0.7$. Curve 3 is calculated with best-fit parameter with $V = 0$ or $V = 1$ (one-shell model).The electrical parameters from intact cells are listed in Table 1.

Table 1. Electrical Parameters of Intact ($p = 0$) Plant Tissue Cells[a]

			best-fit parameters for rebuilding a measured conductivity spectrum										other cell parameters			
tissue	d[b] (μm)	inhomogenity ratio, g	V	S	R_1 (MΩ)	R_2 (MΩ)	R_3 (kΩ)	R_4 (kΩ)	R_5 (kΩ)	R_6 (kΩ)	C_1 (pF)	C_2 (pF)	d_m[c] (nm)	σ_m[d] ($\times 10^8$ S/m)	$\sigma_{vacuole}$ (S/m)	σ_{plasma} (S/m)
carrot	60	0	0.65	0.8	>45	>71	105	3.4	30	450	18	9	4.1	<2.5	0.66	0.53
banana	80	0	0.5	0.7	>48	>94	63	8.4	25	480	25	11	5.2	<1.7	0.54	0.38
potato	100	0	0.7	0.8	>23	>29	70	1.0	13	230	35	20	5.8	<2.5	0.84	0.67
apple	70	0.21	0.6	0.9	>41	>58	714	23	220	410	18	10	5.5	<2.4	0.11	0.10

[a] The absolute value of a best-fit resistance and capacitance was examined for average cell size. The dependence between cell size distribution and electrical parameters was not considered here. [b] Average cell size fixed with light microscopic observation. [c] d_m is the plasma membrane thickness, calculated as $d_m = \epsilon_0\epsilon_m A_m/C_1$, with ϵ_0 the dielectric constant of free space ($\epsilon_0 = 8.85 \times 10^{-12}$ F/m), $\epsilon_m = 2.3$, dielectric constant of membrane phase, and $A_m = d^2$, the membrane area from the average cell in the measurement direction. [d] σ_m is the plasma membrane conductivity, calculated as $\sigma_m = d_m/A_m R_1$.

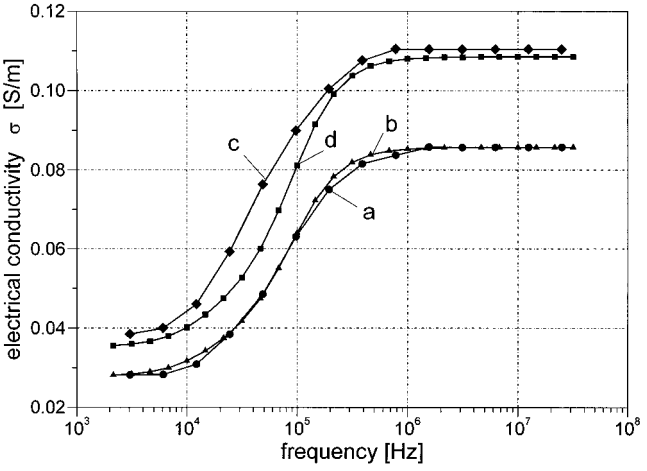

Figure 4. Conductivity spectra of an apple tissue: (a) ●, raw tissue, sample density $\rho = 0.83$ g/cm^3 (the experimental conductivities $\sigma_{3\ kHz} = 0.028$ S/m and $\sigma_{12.5\ MHz} = 0.085$ S/m are used for calculation of curves b and d); (b) ▲, model fitted for untreated tissue with inhomogenity ratio $g = 0.21$ (see Materials and Methods); (c) ♦, measured from sample after high-pressure treatment (at 50 MPa, 10 min), sample density $\rho = 1010$ kg/m^3; (d) ■, predicted for untreated tissue with $g = 0$.

ness, d_m, and membrane conductivity, σ_m, are obtained indirectly and correspond with the data regarding biological membranes cited. For example, the cell membrane thickness is generally assumed to be 5−8 nm, and σ_m is assumed to be 10^{-6}−10^{-10} S/m (*21*, *22*, *28*, *36*, *37*). The most significant accordance of the modulated conductivity spectra with experimental conductivity spectra could be obtained under conditions with relative conductivity of cell contents $S < 1$; i.e., in the plant cell, the ion concentration in the vacuole fluid is higher than that in the plasma ($\sigma_{vacuole} > \sigma_{plasma}$).

Properties of Ruptured Cell Systems. The data obtained experimentally correspond with the data of the model fitted for intact and for predicted disrupted tissues which were ruptured in three different ways (Figure 5).

Typical conductivity spectra of various proportions of intact and disintegrated cells in the measured systems are shown in Figure 5a. Data obtained on samples with partial cell disintegration after mechanical crushing are compared with data on tissue with total cell disruptions after freezing−thawing treatment.

The proportion of disrupted cells, p_o, was determined by eq 23 for coarsely ground tissue and was found to be 0.55 and 0.84, respectively, in fine-grained samples. For the determination of p_o, the experimental conductivities of the untreated and treated samples, σ_l^i, σ_h^i and σ_{lreal}^t, σ_{hreal}^t, were used at frequencies $f_l = 3$ kHz and $f_h = 12.5$ MHz. After a slow freeze−thaw cycle, all cells were completely ruptured, and hence the cell disintegration index was $p_o = 1$.

The rebuilding of measured conductivity spectra for various amounts of disrupted cells in relation to the considered model (system with different portions of intact

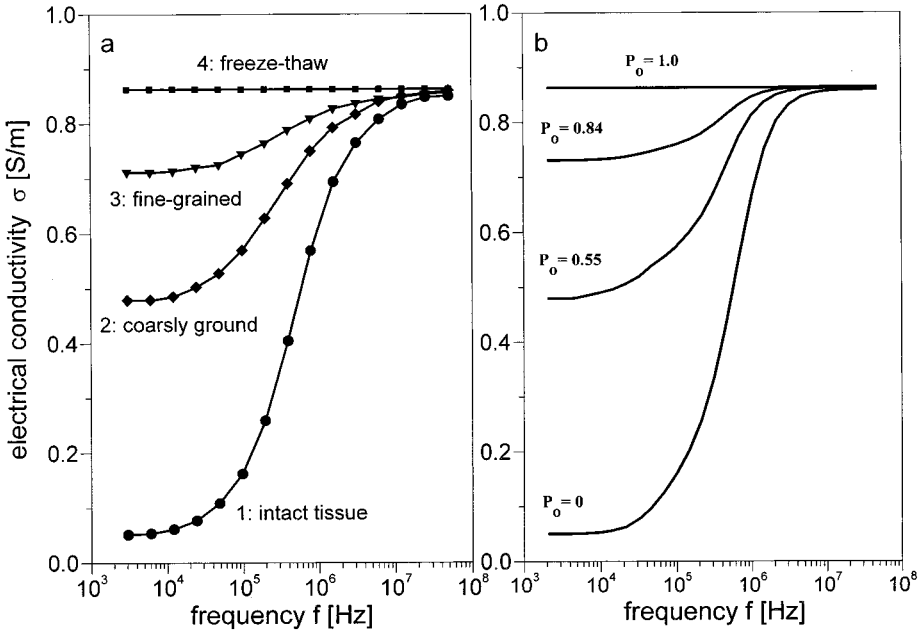

Figure 5. Measured (a) and predicted (b) conductivity spectra of potato tissue after mechanical disruption and freeze−thaw treatment. The ratio of ruptured cells ($p = p_o$) for the calculation of conductivity spectra (eq 1) was determined from the corresponding eq 24 from experimental conductivity of the cell system measured before and after treatment at low (3 kHz) and high (12.5 MHz) frequency.

and ruptured cells) is shown for comparison in Figure 5b. In this case, the procedure for predicting the conductivity spectra of treated samples is the same as that for intact tissue with $p = 0$ (the parameter for intact potato cells is listed in Table 1), but in eq 2, ratios of ruptured cells $p = 0.55$, $p = 0.84$, and $p = 1$ were introduced. The results showed significant resemblance between the experimental data and predicted conductivity spectra used for samples with totally intact or totally ruptured cells as well as for mixed systems consisting of intact and ruptured cells (Figure 5a,b).

This example confirms the fact that the cell disintegration index, p_o, can be calculated from experimental conductivities σ_l^i, σ_h^i and σ_{lreal}^t, σ_{hreal}^t (eq 23), and its appropriateness for the use of the ratio of ruptured cells p in the basic model of cell system is correct.

Application of p_o for Process Characterization. The cell disintegration ratio was determined from plant tissue after mechanical crushing and during drying (*26*). The data obtained on potato and carrot samples show a continuos increase of irreversibly disrupted cells, even during gentle drying (air-drying at 45 °C and velocities 0.5 m/s) treatment. Intact cells were not detectable after drying (up to 20% water content) and rehydration.

The cell disintegration index of potato tissue after thermal treatment (−10 to + 90 °C) is shown in Figure 6. Cell disintegration was not detectable for potato tissue after thermal treatment between −1 and +50 °C. Significant cell permeabilization was observed to begin at freezing temperatures below −1.5 to −2.5 °C and for heat treatment above 54−60 °C.

Continuous impedance measurements allowed the evaluation of the progress of cell membrane permeabilization after treatment. For example, this can lead to essential data on time factors (in seconds after treatment) concerning disruption of plant cells after treatment with one high electric field pulse (HELP) (Figure 7). Within 5 s after pulse treatment, a range of $p_o = 0.22$ was detected and increased within 400 s to a value as high as 0.71.

As a result of energy input of 10.8 kJ/kg during each pulse, the temperature increase in the carrot samples was $\Delta T = 3$ °C. This caused a conductivity increase of

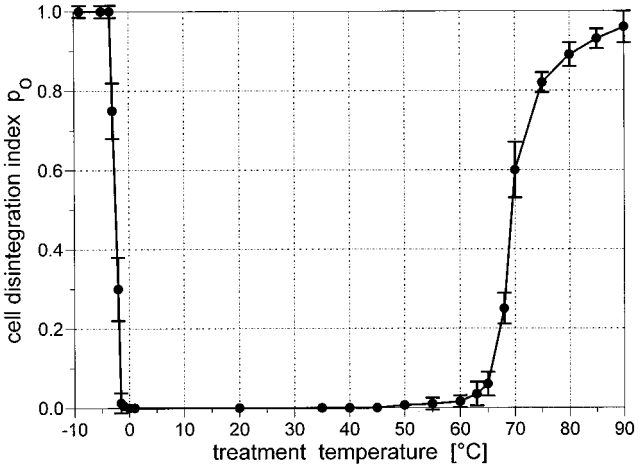

Figure 6. Effects of temperature on cell disintegration index, p_o, in potato tissue. The characteristic conductivities of the intact and treated samples were obtained at 20 °C.

the sample (Figure 7a) in the entire frequency range. The conductivity increase in the frequency range between 3 kHz and about 1 MHz can be explained by the increase in cell membrane permeabilization and the temperature increase (as an example, see the conductivity curve 5 s after pulse application in Figure 7a). The sample conductivity in the range of 2.5−50 MHz was increased purely due to ΔT and reached, during measurements, the initial value (equal to the untreated sample). In the calculation of the disintegration index, the heat-dependent conductivity changes are compensated in eq 23 with the linear coefficient k, and the calculated p_o (Figure 7 b) is effectively the result of only the conductivity changes due to cell permeabilization.

Generally, the parameter p_o is the average cell disintegration characteristic in the sample and describes the transition of a cell from intact to ruptured state. It is known that high-electric-field pulse treatment could cause partial or local destruction of a biological membrane (*38*). Therefore, an approximate value of the extent of cell permeabilization can be inferred from p_o. To obtain

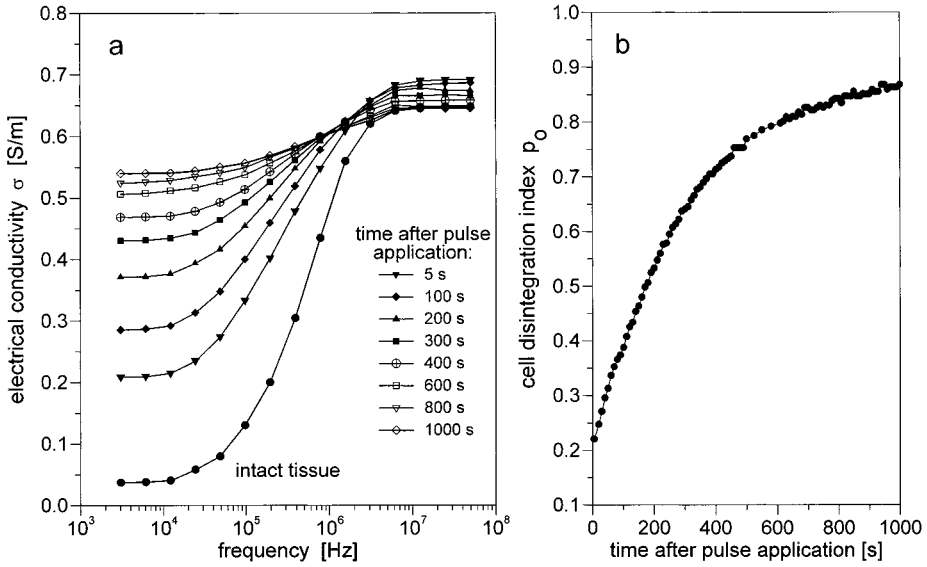

Figure 7. (a) Carrot tissue conductivity spectra (selected curves) measured at various times after application of one high-intensity electric pulse (field strength $E = 3.2$ kV/cm, pulse duration 1.5 ms, temperature rise $\Delta T = 3$ °C). (b) Continuous course of the cell disintegration index p_o versus time after pulse application. For calculation of p_o (eq 24), the measured conductivities in low (3 kHz) and high (12.5 MHz) frequency of the intact and treated tissues were used. The first measurement of conductivity was taken 5 s after the pulse application and then continued at 10-s intervals.

more information about the extent of the cell membrane damage due to high-electric-field pulse treatment, further detailed analysis of the experimental data is required.

The index p_o can also be used as a means of testing the effectiveness of enzymatic treatment on cell membrane disintegration. For example, apple mash was treated with various *Pectinex Ultra SP-L* enzyme concentrations (Figure 8). The initial ratio of the cell disintegration index after mechanical crushing of apple tissue was $p_o = 0.86$; i.e., 14% of the cells in this mash were intact at the start of the experiment. The introduction of endogenous enzymes also leads to membrane permeabilization, which can be seen from the continuously increasing value of p_o during the incubation time for the control sample (see Figure 8).

The data presented show that the addition of a recommend concentration of commercial enzyme did not result in any significant difference of the cell disintegration index from that of the untreated control sample after 1 h (Figure 8, curve 1). Even after the addition of a 150-fold dose of the recommended enzyme concentration, the maximum cell disintegration index was reached only after 4−5 h of treatment. This lag period is considerably higher than the recommended optimum treatment time of 0.5−1 h at 20 °C (*39*). For comparison, the possible rapid process of destruction of the plant membrane shows the cell disintegration kinetic of the same apple mash upon addition of alcohol at a concentration of 150 g/kg (Figure 8). The membrane disruption process after alcohol treatment led to complete disintegration of cell system within 30 min.

The frequency dependence of the conductivity, as a result of charging polarization of an insulated cell membrane in an electrical field, is a phenomenon in practically all biological cell systems. The parameter p_o discussed here characterized the transformation degrees from the insulation to the conduction state of an elementary unit of the sample, relating to some initial state of the cell system (in this work, the intact tissue was used as the initial condition).

The definition of p_o follows from the relative changes of sample conductivities, which were obtained at low- and high-frequency ranges. In this characteristic frequency

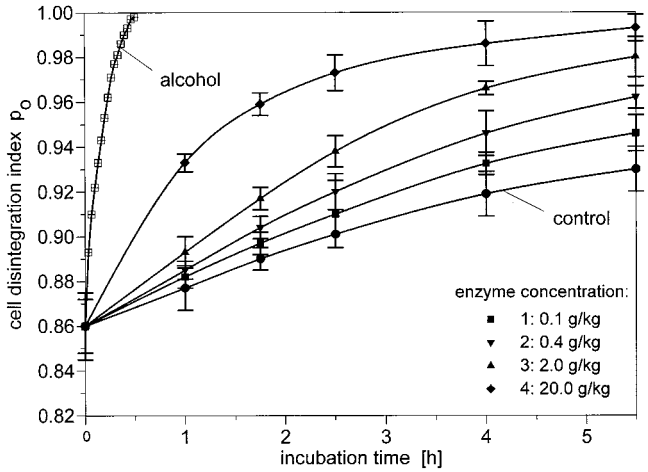

Figure 8. Kinetics of the cell disintegration of apple mash during enzyme treatment (temperature 20 °C) with various *Pectinex Ultra SP-L* enzyme dose levels (curves 1−4). Curve □: apple mash treated with 96% alcohol in concentration 150 g/kg. The manufacturer's recommendation for the optimal treatment condition of the enzyme for apple mash was as follows: dose level 0.08−0.13 g/kg, 15−25 °C, 0.5−1 h, no stir (*39*).

range, the electrical behavior of cells could be abstracted from a suitable cell model, and consequently, the cell disintegration index can be considered as a reliable and accurate indicator for the cell disintegration of various biological materials, independent of their morphological structure. As previously discussed, it is important that the experimental conductivities in eq 23 be determined in the characteristic low- (f_l) and high-frequency (f_h) regions.

Based on these results, this method has been applied to detect cell disruption due to various processing operations in various plant and animal tissues as well as in individual plant cells in cell suspensions. As for the examples, the postmortem pattern of membrane disassembly in animal muscle tissue (characteristic frequencies about $f_l \leq 3$ kHz and $f_h \geq 25$ MHz (*26*)) as well as the membrane disintegration of animal and fish tissue (for trout fillet, $f_l \leq 3$ kHz and $f_h \geq 3$ MHz) was registered

after mechanical disruption, freezing−thawing, and HELP treatment. The evaluation of membrane rupture in yeast cell suspension (*S. ceriviase*, average cell size 6 μm, $f_l \leq$ 50 kHz and $f_h \geq$ 80 MHz) and potato cell culture after HELP treatment was performed using this method.

The cell disintegration index can be considered as a reliable and accurate indicator for the cell permeabilization of biological materials. Based on the results obtained so far, the cell disintegration index is applied routinely in our laboratory for optimization of the high-electric-field pulse process parameters as well as for the evaluation of the effectiveness of other permeabilization/disintegration processes (*26*, *40*).

The cell disintegration index, p_o, seems appropriate to quantify the conditions of cell systems, and it is important for optimization of various food processes (i.e., minimizing cell damage in minimal processes, monitoring disruption for mass transfer purposes, and inducing biosynthetic reactions/responses).

Conclusion

A study of the electrical behavior of intact cells with insulated biological membrane led to the analysis of morphological and structural properties of the cell systems. Based on an equivalent circuit model of an individual cell, the frequency-dependent electrical conductivity of the untreated and treated plant cell systems with different ratios of intact, ruptured cells and extracellular compartments could be predicted in a range of the β-dispersion frequency.

A method is presented for the accurate determination of the degree of cell permeabilization (cell disintegration index, p_o), based on the relative changes of sample conductivities, which were obtained at characteristic low- and high-frequency ranges of the β-dispersion (frequencies f_l lower than 5 kHz and f_h higher than 5 MHz valid for most vegetable tissues). The parameter p_o characterized the transformation degrees from the insulation to the conduction state of an elementary unit of the sample, which is the average cell, relating to the initial state of the cell system.

This simple and more or less nondestructive method could be very valuable for the prediction of the behavior of biological cells in terms of the cell disruption during processing, storage, and consumption of food materials with cellular structure. In addition, an example of practical application of cell disintegration index for process characterization was shown.

Acknowledgment

This work has been supported by grants from the FEI (Forschungskreis der Ernährungsindustrie e.V., Bonn), the AiF (Project No. FV 10611N), and the German Ministry of Economics as well as by the European Commission (FAIR contract CT97-3044).

References and Notes

(1) Knorr, D. Plant cell and tissue cultures as model systems monitoring the impact of unit operations on plant foods. *Trends Food Sci. Technol.* **1994**, *5*, 328−331.

(2) Maxwell, J. C. *Arteriese on Electricity and Magnetism*, 3rd ed.; Clarendon Press: Oxford, 1891; Vol. I, Chapter IX, p 435.

(3) Wagner, K. W. Erklärung der dielektrischen Nachwirkungsvorgänge auf Grund Maxwellscher Vorstellungen. *Arch. Elektrotech. (Berlin)* **1914**, *2*, 371.

(4) Dänzer, H. Über das Verhalten biologischer Körper im Hochfrequenzfeld. *Ann. Phys.* **1934**, *20*, 463−480.

(5) Rajewsky, B. Biophysikalische Grundlagen der Ultrakurzwellenwirkung im lebenden Gewebe. In Ergebnisse der biophysikalischen Forschung in Einzeldarstellungen, Bd. 1, Ultrakurzwellen; Rajewsky, B., Ed.; Georg Thieme Verlag: Leipzig, 1938; p 77.

(6) Cole, K. S. Impedance of single cells. *Tabulae Biologicae* 19 (Cellula); Den Haag: Berlin, 1942; Part 2, p 24.

(7) Fricke, B. H. The complex conductivity of a suspension of stratified particles of spherical or cylindrical form. *J. Phys. Chem.* **1955**, *59*, 168−170.

(8) Pauly, H.; Schwan, H. P. Über die Impedanz einer Suspension von kugelförmigen Teilchen mit einer Schale. *Z. Naturforsch.* **1959**, *14b*, 125−131.

(9) Pauly, H. Über die elektrische Kapazität der Zellmembran und die Leitfähigkeit des Zytoplasmas von Ehrlich-Aszitestumuorzellen. *Biophysik (Berlin)* **1963**, *1*, 143−153.

(10) Schwan, H. P. Field interaction with biological matter. *Ann. N. Y. Acad. Sci.* **1977**, *303*, 198−213.

(11) Zhang, M. I. N.; Willison, J. H. M. Electrical impedance analysis in plant tissue: The effect of freeze−thaw injury on the electrical properties of potato tuber and carrot root tissue. *Can. J. Plant Sci.* **1992**, *72*, 545−553.

(12) Zhang, M. I. N.; Willison, J. H. M. Electrical impedance analysis in plant tissue: *in vivo* detection of freezing injury. *Can. J. Bot.* **1992**, *70*, 2254−2258.

(13) Stout, D. G.; Hall, J. W.; Mclaughlin, N. B. *In vivo* plant impedance measurements and characterization of membrane electrical properties: The influence of cold acclimation. *Cryobiology* **1987**, *24*, 148−162.

(14) Repo, T.; Tuovinen, T.; Savolainen T. Estimation of an electrical model of plant tissue using the impedance logus. *Silva Carelica* **1990**, *15*, 51−59.

(15) Greenham, C. G.; Helms, K.; Müller, W. J. Influence of virus infections on impedance parameters. *J. Exp. Bot.* **1978**, *29*, 867−877.

(16) Hennings, C. Ein neues elektronisches Schnellvervahren zur Ermittlung der Frische von Seefischen. *Z. Lebensm. Untersuch. Forsch.* **1962**, *119*, 461−477.

(17) Charpentier, J.; Goutefongea, R.; Sale, P.; Thomasset, A. La discrimination des viandes fraiches et congelees par mesures d'impedance a deux frequences. *Ann. Biol. Anim. Biochem. Biophys.* **1972**, *12*, 173−178.

(18) Ehlermann, D. Beurteilung von Lebensmitteln aufgrund elektrischer Eigenschaften. *Mitt. Geb. Lebensm. Hyg.* **1979**, *70*, 107−116.

(19) Pliquett, F.; Pliquett, U.; Schöberlein, L.; Freywald, K. Impedanzmessungen zur Charakterisierung der Fleischbeschaffenheit. *Fleischwirtschaft* **1995**, *75*, 496−498.

(20) Schwan, H. P. Electrical properties of tissue and cell suspensions. In *Advances in Biological and Medical Physics*; Laurence, J. H., Tobias, C. A., Eds.; Academic Press: New York, 1957; Vol. 5, pp 147−209.

(21) Zimmermann, U. Electric field-mediated fusion and related electrical phenomena. *Biochim. Biophys. Acta* **1982**, *694*, 227−277.

(22) Pauly, H. Die Struktur der zytoplasmatischen Membran. *Biophysik* **1964**, *1*, 347−358.

(23) Nelson, S. O.; Forbus, W. R.; Lawrence, K. C. Microwave permittivities of fresh fruits and vegetables from 0.2 to 200 GHz. *Trans. Am. Soc. Agric. Eng.* **1993**, *37*, 183−189.

(24) Hayden, R. I.; Moyse, C. A.; Calder, F. W.; Crawford, D. P.; Fensom, D. S. Electrical impedance studies on potato and alfalfa tissue. *J. Exp. Bot.* **1969**, *20*, 177−200.

(25) Zhang, M. I. N.; Willison, J. H. M. Electrical impedance analysis in plant tissue: A double shell model. *J. Exp. Bot.* **1991**, *42*, 1465−1475.

(26) Angersbach, A.; Heinz, V.; Knorr, D. Elektrische Leitfähigkeit als Mass des Zellaufschlussgrades von zellulären Materialien durch Verarbeitungsprozesse. *Lebensm. Verpackungstechnik.* **1997**, *42*, 195−200.

(27) Shaw, T. M.; Galvin, J. A. High-Frequency-Heating Characteristics of Vegetable Tissues Determined from Electrical-Conductivity Measurements. *Proc. I.R.E.−Waves Electrons Sect.* **1949**, *37*, 83−86.

(28) Marszalek, P.; Zielinsky, J. J.; Fikus, M.; Tsong T. Y. Determination of electrical parameters of cell membranes by a dielectrophoresis method. *Biophys. J.* **1991**, *59*, 982−987.

(29) Schwan, H. P. Determination of biological impedance. In *Physical techniques in biological research*; Nastuk, W. L., Ed.; Academic Press, Inc.: New York, 1963; Vol. 6, part B, p 323.
(30) Schwan, H. P. Electrode polarization impedance and measurements in biological materials. *Ann. N. Y. Acad. Sci.* **1968**, *148*, 191−209.
(31) Marquard, D. W. An algoritm for least squares estimation of non-linear parameters. *J. Soc. Ind. Appl. Math.* **1963**, *11*, 431−441.
(32) Wiliams, E. J.; Johnston, R. J.; Daintly, J. The electrical resistance and capacitance of the membranes of *Nitellla translucens*. *J. Exp. Bot.* **1964**, *15*, 1−14.
(33) Wang, H. C.; Li, J. S. The difference in freezing tolerance between protoplast and vacuole of wheat leaves. In *Plant Biology. Vol. 5. Plant cold hardiness*; Li, P. H., Ed.; Alan R. Liss: New York, 1987; pp 221−228.
(34) Dörnenburg, H.; Knorr, D. Cellular permeabilization of cultured plant tissues by high electric field pulses of ultra high pressure for the recovery of secondary metabolites. *Food Biotechnol.* **1993**, *7*, 35−48.
(35) Mönch, S.; Knorr, D. Influence of high-intensity electric field pulses treatment of plant cells suspension. Berlin University of Technology (unpublished data), 1997.
(36) Szabo, G. Electrical characteristics of ion transport in lipid bilayer membranes. *Ann. N. Y. Acad. Sci.* **1977**, *303*, 266−280.
(37) Kuang, W.; Nelson S. O. Low-frequency dielectric properties of biological tissues: A review with some new insights. *Trans. Am. Soc. Agric. Eng.* **1998**, *41*, 173−184.
(38) Ho, S. Y.; Mittal, G. S. Electroporation of cell membranes: A review. *Crit. Rev. Biotechnol.* **1996**, *16*, 349−362.
(39) Bussmann, J. Innovativer Enzymeinsatz in der Früchteverarbeitung−eine Zukunfttechnologie. *Flüssiges. Obst.* **1992**, *59*, 411−414.
(40) Knorr, D.; Angersbach, A. Impact of high-intensity electrical field pulses on plant membrane permeabilization. *Trends Food Sci. Technol.* **1998**, *9*, 185−191.

Accepted May 28, 1999.

BP990079F